Scientific Reports

https://doi.org/10.1038/s41598-026-41962-w

Article in Press

Study on the structural characteristics of nitrogen-containing compounds in co-pyrolysis tar of low rank coal using ^{1}H-^{15}N HMBC analysis

Received: 12 October 2025

Accepted: 24 February 2026

Published online: 06 March 2026

Cite this article as: Zhang Y., Chen P., Shi G. *et al.* Study on the structural characteristics of nitrogen-containing compounds in co-pyrolysis tar of low rank coal using ^{1}H-^{15}N HMBC analysis. *Sci Rep* (2026). https://doi.org/10.1038/s41598-026-41962-w

Yichen Zhang, Peiqi Chen, Guantao Shi, Nai Wang, Haining Tian, Gang Li, Bin Su, Xiang Han, Anning Zhou, Qiuhong Wang, Zhenmin Luo & Fuxin Chen

Study on the structural characteristics of nitrogen-containing compounds in co-pyrolysis tar of low rank coal using ^{1}H-^{15}N HMBC analysis

Yichen Zhang[1,+], Peiqi Chen[1,+], Guantao Shi[2], Nai Wang[2], Haining Tian[2], Gang Li[1], Bin Su[3], Xiang Han[1], Anning Zhou[1], Qiuhong Wang[3], Zhenmin Luo[3], Fuxin Chen[1,*]

[1]College of Chemistry and Chemical Engineering, Xi'an University of Science and Technology, Xi'an 710054, China
[2]Changqing Industrial Group Co., Ltd., Xi'an 710016, China
[3]College of Safety and Engineering, Xi'an University of Science and Technology, Xi'an 710054, China

[*]corresponding.author chenfuxin@xust.edu.cn or chenfuxin1981@163.com
[+]these authors contributed equally to this work

ABSTRACT

Clarifying the structure, category, and content of nitrogen-containing compounds in coal tar is not only the key to directional regulation of pyrolysis processes, but also one of the needs for refined utilization of coal resources. developing simple, direct, and efficient structural analysis methods for nitrogen-containing compounds is very important for further investigation of nitrogen-rich tar. In this study, nitrogen-rich tar was obtained by co-pyrolysis through low rank coal and NH_4Cl; meanwhile, $^{15}NH_4Cl$ were selected as the NMR signal enhancement for the structural characteristics research. The results indicated that the nitrogen-rich tar primarily consisted of substituted aromatic amines, aliphatic amines, piperidine, pyrrole, pyridine, quinoline, and other nitrogen-containing compounds. Various nitrogen-containing compounds exhibit distinct functional properties. Compared with GCMS analysis method, ^{1}H-^{15}N HMBC NMR provides more structural information about nitrogen-containing compounds, especially the substitution characteristics of aromatic amines; at the same time, ^{1}H-^{15}N HMBC provides very "clean" 2D spectrum compared to ^{1}H-^{13}C HSQC simultaneously.

Introduction

Nitrogen-containing compounds represent an important class of organic compounds that are widely found in animals, plants, and natural products[1,2]. Due to their high biological activity, efficient systemic absorption, and low toxicity, these compounds are frequently employed as structural motifs in pharmaceuticals and agrochemicals, and are therefore extensively utilized across various fields, including medicine[3-5], fuel[6,7], dyes[8], materials[9], and food additives[10]. In the field of chemical engineering, coal tar serves as a significant natural source of nitrogen-containing heterocycles[11], particularly pyridine, quinoline, carbazole, and acridine. With the continuous advancement of modern industry, simple nitrogen-containing compounds such as aniline and pyridine[12] can now be efficiently synthesized through petrochemical processes. However, structurally complex nitrogen-containing heterocyclic compounds, such as carbazole and acridine and their derivatives, remain challenging to produce at large scale in an economically viable and technically feasible manner due to the high cost and low efficiency associated with conventional synthetic methods. Therefore, as a natural resource abundant in complex nitrogen-containing heterocyclic compounds, coal tar continues to face significant challenges in its high-value utilization and efficient analysis.

Coal tar contains a diverse range of nitrogen-containing compounds with a high total quantity, but individual components are present in relatively low concentrations. The occurrence forms and removal mechanisms of these compounds require further investigation, and current qualitative and quantitative analytical methods remain insufficiently developed. The separation and enrichment of nitrogen-containing compounds, along with the accurate identification of their composition and

structure, have become key challenges in the field of coal tar processing and utilization[13]. Currently, the primary methods for identifying the composition of nitrogen-containing compounds in tar include gas chromatography (GC), gas chromatography-mass spectrometry (GC/MS), Fourier transform infrared spectroscopy (FT-IR), and nuclear magnetic resonance (NMR) techniques[14,15]. The GC/MS analyzer combines the separation capability of chromatography with the qualitative advantages of mass spectrometry, enabling rapid and accurate analysis of multi-component mixtures within a relatively short time frame. Although it offers advantages such as high specificity, minimal sample requirements, fast analysis speed, and high sensitivity. However, the compounds present in coal tar possess complex structures, and multiple isomers are often present, which exhibit highly similar structural features and their mass spectra are also extremely similar, which means that it poses a great challenge for GC/MS analysis of isomers. For instance, He et al.[16] reported nearly identical mass spectral data for quinoline and cinnamoyl nitrile when analyzing the pyrolysis products of cinnamic acid and ammonium chloride using GC/MS. For known nitrogen-containing compounds, identification can be accomplished by comparing their retention times with those of reference standards. However, for structurally complex and unknown nitrogen-containing compounds, additional analytical techniques must be employed in combination to achieve accurate identification.

Nuclear magnetic resonance has a very strong ability to identify isomers, capable of distinguishing structural isomers, cis-trans isomers and enantiomers. Since most isomers (except enantiomers) have structural and spatial differences, the atomic nuclei and the local environment of the magnetic field are different, often presenting different chemical shifts, coupling constants and peak splitting patterns. As coal tar is a complex mixture, direct ^{1}H NMR and ^{13}C NMR detection often result in severe signal overlap, leading to the loss of critical structural information[17]. The application of ^{15}N NMR can circumvent the complex chemical environments of hydrogen and carbon atoms, enabling direct detection of nitrogen atoms and thus providing more direct insights into molecular structure[18]. However, several challenges may arise in ^{15}N NMR analysis. Firstly, coal tar contains a diverse range of nitrogen compounds, many of which are present at relatively low concentrations. Additionally, the natural abundance of ^{15}N is very low (approximately 0.37%), and the quadrupole coupling effect of ^{14}N further complicates the measurement. These factors can collectively contribute to the loss of spectral signals in ^{15}N NMR[19]. The application of ^{15}N labeling can significantly enhance signal intensity, thereby enabling clearer characterization of molecular structures. For example, Ramirez et al. successfully enhanced the nitrogen signal in amino acids using ^{15}N-labeled amino acids[20]. However, in coal tar, many nitrogen atoms often exhibit similar chemical environments, resulting in severe signal overlap. Two-dimensional (2D) NMR techniques, such as ^{1}H-^{15}N HSQC and ^{1}H-^{15}N HMBC can enable clearer signal assignments within a shorter time frame, reduce both experimental time and sample consumption, and elucidate the direct connectivity between hydrogen and nitrogen atoms[21]. For the identification of isomers, the ^{1}H-^{15}N HMBC technique is superior to the GC/MS technique. For instance, as mentioned earlier, the mass spectra of quinoline and cinnamic anhydride are exactly the same, but due to the different chemical environments of the N atom, the ^{1}H-^{15}N HMBC spectra of the two are significantly different.

Based on the aforementioned experimental research, Hongliulin rich oil coal was selected as the raw material and co-pyrolyzed with NH_4Cl and $^{15}NH_4Cl$, respectively, to produce nitrogen-rich tar. Due to the diversity and complexity of nitrogen-containing compounds present in the tar, a method for rapidly screening nitrogen-containing functional groups using ^{1}H-^{15}N HMBC NMR spectra was developed. The use of rich oil coal as a carbon source offers advantages such as low cost and wide availability, thereby increasing the added value of coal. The complex structure of coal provides a variety of precursors, which is beneficial for the formation of C-N bonds. Through nitrogen doping and pyrolysis reactions, the utilization efficiency of coal tar has been improved, breaking away from traditional synthesis methods for nitrogen-containing compounds and offering valuable insights for the deep processing and comprehensive utilization of coal tar[22]. This approach holds considerable scientific and practical significance. Therefore, the establishment of a rapid and effective analytical method for nitrogen-containing compounds is of substantial importance.

Results and Discussion

NMR Analysis

^{1}H-^{15}N HMBC Results of Diverse Nitrogen-Containing Compounds

It is well established that the nitrogen-rich tar obtained from the co-pyrolysis of oil-rich coal and NH4Cl possesses an exceptionally complex composition. For nitrogen (N), the chemical environment is less complex compared to hydrogen (H) and carbon (C), yet the signals from various nitrogen-containing compounds still exhibit overlap and interference. Initially, one-dimensional ^{15}N NMR analysis was performed on the coal tar, revealing no detectable peaks. This discrepancy may be attributed to the inherently low sensitivity of one-dimensional ^{15}N NMR, which requires high concentrations of nitrogen-containing compounds for effective signal detection. However, even though nitrogen-rich tar contains a relatively high overall abundance of such compounds, the relative concentration of each individual species remains low, which critically hinders signal detection. The ^{1}H-^{15}N HMBC (Heteronuclear Multiple Bond Correlation) spectrum correlates ^{1}H nuclei with remotely coupled ^{15}N nuclei, typically showing coupling information between protons separated by two to three bonds and their associated nitrogen atoms. This two-dimensional NMR technique facilitates more detailed identification of nitrogen-containing compound types. Given the structural diversity and uncertain configurations of nitrogenous compounds in nitrogen-rich tar, reference compounds containing various nitrogen functional groups were analyzed prior to the examination of the tar sample. Their corresponding ^{1}H-^{15}N coupling signal chemical shift data are summarized in Table 1.

Table 1. Chemical Shifts of ^{1}H-^{15}N Coupling Signals for Ten Distinct Nitrogen-Containing Compounds.

No.	Compound	δ_H (ppm)	δ_N (ppm)
1	Ethylamine	0.98、2.57	29.2
2	Dicyclohexylcarboimide	1.26、1.83	102.4
3	N, N-dimethylformamide	2.66、7.67	105.6
4	Aniline	7.25、7.46	88.1
5	α -naphthylamine	6.86	53.8
6	Pyrrole	6.99、6.58	146.4
7	Pyridine	7.22、8.60	312.9
8	Quinoline	7.26、8.09、8.83	317.5
9	Acetonitrile	2.00	244.9
10	5, 5-dimethyl-1-pyrroliroin-N oxide	1.18、1.90、2.35、6.57	311

To enhance the differentiation of various nitrogen-containing functional groups, a classification strategy was applied for their identification. As shown in Figure 1, the vertical axis represents the chemical shift of nitrogen atoms, and the horizontal axis denotes the chemical shift of hydrogen atoms. The two-dimensional spectrum was divided into four quadrants using δ_H = 4 ppm and δ_N = 200 ppm as boundary thresholds. The ^{1}H-^{15}N coupling signals of nitrogen-containing compounds listed in Table 1 are distributed across various quadrants in first quadrant in Figure 1. The first quadrant represents coupling signals between nitrogen atoms in the high-field region and hydrogen atoms in the high-field region, including certain amines, imines, azo compounds, and N-alkyl-substituted amides, as illustrated in first quadrant in Figure 1. Hydrogen atoms in this region are characterized by the absence of direct attachment to highly electronegative groups or aromatic rings, whereas nitrogen atoms may be bonded to strongly electronegative groups such as carbonyl moieties. Due to the relatively small electronegativity difference between the coupled nuclei, the nitrogen chemical shifts remain below δ_N = 200 ppm (corresponding to the second quadrant in Figure 1), even when deshielded. However, attachment to multiple electronegative groups may potentially result in chemical shifts exceeding this threshold. The second quadrant represents the coupling between nitrogen atoms in the high-field region and hydrogen atoms in the low-field region, as exemplified by compounds such as anilines, diphenylamines, naphthylamines, pyrroles, and formamides, as shown in second quadrant in Figure 1. This region is primarily characterized by aromatic amines, where the hydrogen atoms are bonded to highly electronegative groups or directly to aromatic systems, including carbonyl groups, benzene rings, and pyrrole rings. The third quadrant exhibits a chemically opposite atomic environment compared to the first quadrant, with

both hydrogen and nitrogen atoms located in the low-field region. This region is predominantly composed of six-membered aromatic nitrogen heterocycles such as pyridine and pyrimidine rings, as shown in third quadrant in Figure 1. The chemical environment of hydrogen atoms in this area is similar to that observed in the second quadrant; however, due to inductive effects, conjugation, and anisotropic influences arising from the six-membered aromatic nitrogen heterocycles, the chemical shifts of nitrogen atoms are significantly higher than those observed in pyrrole structures. A subset of compounds includes non-azacyclic structures, such as nitro groups, oximes, and nitrogen oxides, in which the nitrogen atoms are directly bonded to highly electronegative groups or atoms, resulting in upfield shifts of their chemical shifts. Furthermore, cyano groups exhibit elevated nitrogen chemical shifts due to the sp hybridization of the nitrogen atom, leading to coupling signals observed in the low-field region of the nitrogen spectrum. The chemical environment of nitrogen atoms in the fourth quadrant is similar to that of the third quadrant, while the hydrogen environment corresponds to that of the first quadrant specifically, nitrogen atoms in third-quadrant compounds have nearby alkyl substituents. Coupling signals in the fourth quadrant appear exclusively when substituents containing high-field hydrogen atoms replace low-field hydrogen atoms adjacent to nitrogen, as shown in forth quadrant in Figure 1.

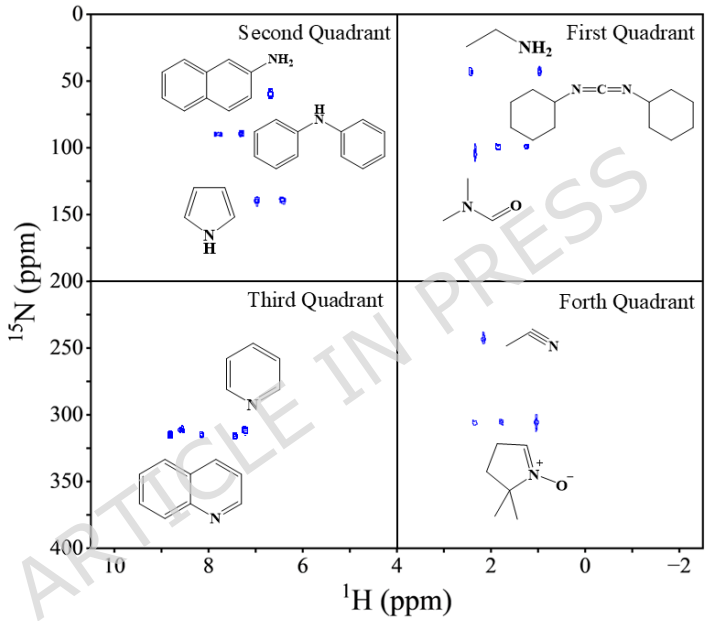

Figure 1. The ^{1}H-^{15}N HMBC NMR signal distribution map of various nitrogen-containing compounds (divided into four quadrants with δ_H = 4 ppm and δ_N = 200 ppm as boundaries).

Characterization of Nitrogen-Containing Compounds in Tar by ^{1}H-^{15}N HMBC Analysis

Based on the peak emergence patterns of atoms in different chemical environments across various field regions, a methodology has been developed for the rapid identification of nitrogen-containing functional groups in ^{1}H-^{15}N HMBC NMR spectra. This approach offers both a theoretical foundation and practical guidance for the efficient structural characterization of nitrogenous compounds in tar and other complex mixtures. Figure 2 presents the ^{1}H-^{15}N HMBC NMR spectrum of co-pyrolysis products obtained from oil-rich coal and $^{15}NH_4Cl$. Spectral analysis reveals that the majority of nitrogen-containing compounds derived from the co-pyrolysis process are distributed in the first and fourth quadrants. Figure 3 is an enlarged view of the first quadrant in Figure 2, the ^{1}H-^{15}N coupling signals are predominantly concentrated within the 50-190 ppm range, with most signals appearing between 50 and 85 ppm. Based on the signal characteristics in the first quadrant of Figure 1 and the speculation of the signal, it can be preliminarily inferred that the nitrogen-rich tar contains aliphatic amines and piperidine derivatives[23]. Because there are a lot of aliphatic hydrocarbon compounds in coal, they originate from the lipid organic matter in the remains of coal-forming plants. For example, algae, roots, stems and leaves of higher plants contain a large amount of aliphatic compounds. When coal undergoes pyrolysis, the large molecular structure of coal breaks down to generate long-chain alkyl groups, and the side chains also break down to form short-chain alkyl groups such as methyl and ethyl. Subsequently, these alkyl groups combine with amino groups

to produce various amine compounds. The piperidine compounds may be related to the presence of cellulose, hemicellulose and lignin in coal, which are all six-membered oxygen-containing rings found in biomass. Under high temperatures, they will undergo complex radical exchange reactions with amino free radicals, thereby generating various six-membered nitrogen-containing rings.[24]. In addition, signals are also observed within the 110-190 ppm range, where the chemical shift of nitrogen atoms is elevated, indicating a decrease in electron cloud density around the nitrogen atom and a reduced shielding effect. These characteristics are consistent with those of pyrrole. However, as shown in Figure 1, the signal of pyrrole is usually in the second quadrant, the observed signals likely correspond to α-alkyl-substituted pyrrole derivatives (bearing one or multiple alkyl groups). According to previous studies, coal tar contains furan compounds, and their main source is also related to the biomass in coal. When cellulose undergoes pyrolysis, it generates intermediates such as left-handed glucans through transglycosylation reactions[25]. The furan compounds are mainly obtained through further decomposition caused by competitive reactions and secondary decomposition of left-handed glucans during the formation process of left-handed glucans[26]. These furan compounds react with amino radicals to form various five-membered nitrogen heterocycles. Signals are detected in the second quadrant, although not abundantly, and are primarily concentrated within the 50-80 ppm range. Based on the signal comparison in the second quadrant of Figure 1, it can be concluded that the compounds in this area are likely to be aniline or naphthylamine compounds. As is well known, coal tar contains significant amounts of benzene and naphthalene derivatives. Under the experimental conditions used, hydrogen atoms on these compounds, particularly those located on aromatic rings, are converted into hydrogen radicals, which subsequently participate in exchange reactions with amino radicals to form aromatic amine compounds.

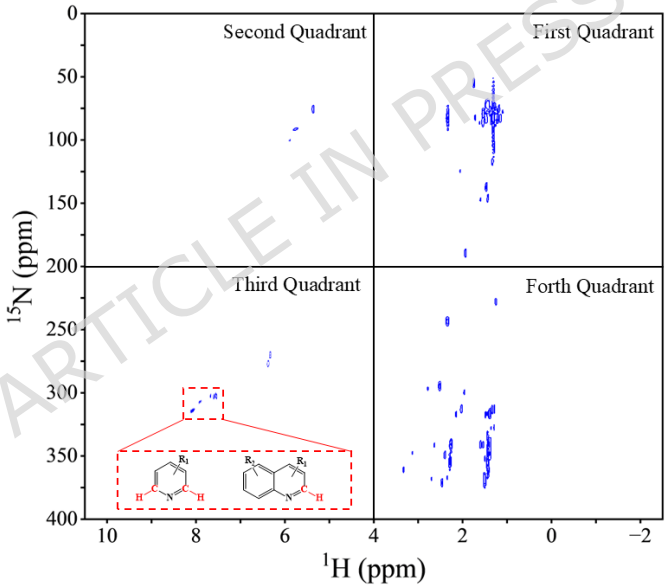

Figure 2. The ^{1}H-^{15}N HMBC NMR Spectra of Co-Pyrolysis Products Derived from Oil-Rich Coal and NH_4Cl (The Spectral Data Are Partitioned into Four Quadrants Using δ_H = 4 ppm and δ_N = 200 ppm as Demarcation Thresholds).

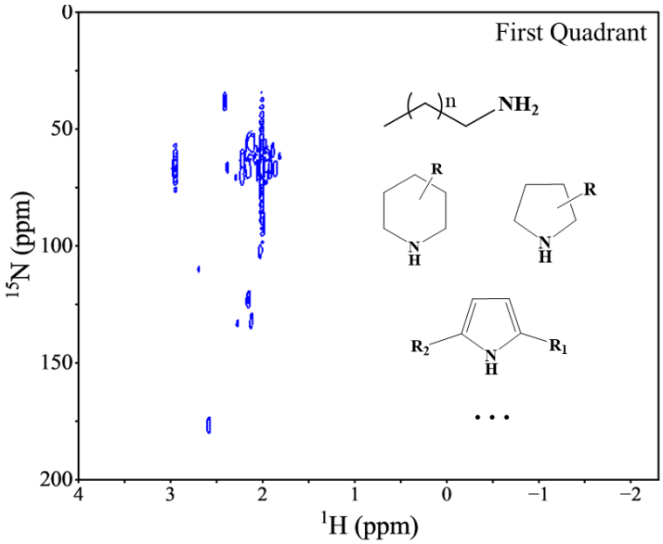

Figure 3. Enlarged View of the First Quadrant in Figure 2.

For the third and fourth quadrants, the majority of coupling signals are located in the fourth quadrant. Comparing the signals in the third quadrant of Figure 1, the coupling signals of pyridine and quinoline derivatives were identified in the third quadrant, as indicated by the red box in Figure 2. The signals in the fourth quadrant display greater complexity. As illustrated in Figure 4, upon magnification of this region, the signals are predominantly clustered within the 300–400 ppm range. This suggests a further reduction in the electron cloud density surrounding the nitrogen atoms, a characteristic commonly associated with all six-membered nitrogen heterocyclic derivatives. Similar to pyrrole, these coupling signals would typically be observed in the third quadrant. Therefore, this region mainly contains signals originating from α-alkyl-substituted pyridine, pyrazine, and pyridazine derivatives. For pyrrole, although its electron cloud density is higher than that of pyridine, if the nitrogen atom is bonded to an oxygen atom to form an oxidized nitrogen species, the electron density may be drawn toward the oxygen atom, potentially leading to chemical shifts in this region. Consequently, this region may also include N-oxidized pyrroline derivatives. The primary sources of these nitrogen-containing compounds are the oxygen-containing heterocycles originally present in coal tar. These compounds undergo complex chemical reactions with amino radicals at elevated temperatures. Given the bond energy of the C-O bond and the conjugation effects of electrons on oxygen atoms, only a portion of the oxygen atoms react with amino radicals. Nevertheless, this fraction of nitrogen-containing compounds is sufficient to be detected by nuclear magnetic resonance spectroscopy. Additionally, a limited number of signals were observed within the 200-300 ppm range. As shown in the signal in the fourth quadrant of Figure 1, these signals may originate from cyano groups. He et al.[16] demonstrated through the co-pyrolysis of cinnamic acid and ammonium chloride that carboxyl groups react with amino radicals to form amides, which subsequently undergo dehydration under specific conditions to yield cyano groups. Therefore, the cyano signals could arise either from the reaction between carboxyl compounds and amino radicals present in coal tar, or alternatively from intrinsic nitrile compounds within the coal tar itself. Moreover, a minor signal persists within the 350-400 ppm range, likely attributable to the presence of strong electron-withdrawing groups adjacent to the nitrogen atoms in the aforementioned structures, resulting in an upfield chemical shift of the nitrogen nuclei. Additionally, coupled signals are observed in the 200-250 ppm region, where the electron density displays intermediate characteristics between pyrrole and pyridine. Based on established spectroscopic principles, this region indicates the potential presence of cyanide-substituted compounds.

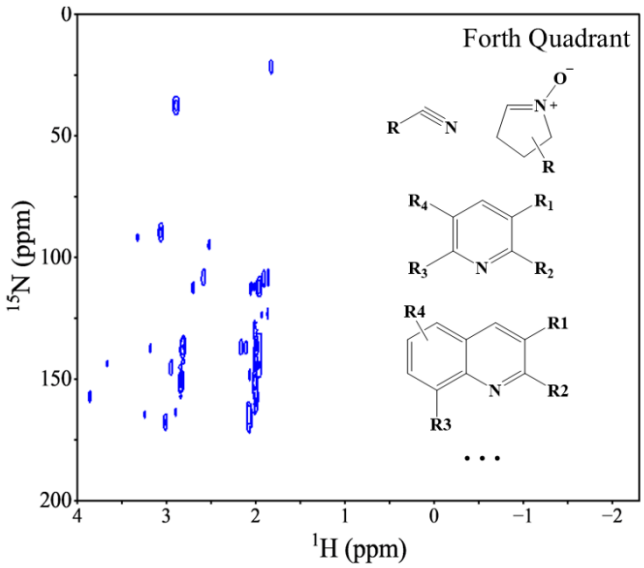

Figure 4. Enlarged View of the Fourth Quadrant in Figure 2.

Results of ^{1}H-^{13}C NMR

Although the environment of H and C atoms in coal tar is complex, some special coupling signals can still be found to identify some compounds in pyrolysis products[27]. However, it is simply impossible to distinguish the specific structures of nitrogen-containing compounds by ^{1}H NMR alone. As an initial approach, ^{1}H-^{13}C HSQC spectroscopy was utilized to detect directly bonded ^{1}H-^{13}C pairs, thereby revealing direct carbon–hydrogen connectivity[28]. The spectra were acquired using a 400 MHz Bruker Avance III HD spectrometer with the HSQCEDETGPSISP pulse sequence, employing 8 scans and 16 dummy scans. Figure 5 displays the ^{1}H-^{13}C HSQC spectrum of the nitrogen-rich tar, in which coupling signals for both hydrogen and carbon nuclei are observed across both the downfield and upfield regions. Empirical evidence indicates that the downfield coupling signals primarily arise from benzene ring structures, suggesting the presence of unsubstituted aromatic compounds within the nitrogen-rich tar. For aromatic compounds, the δ_C values typically appear around 130 ppm. Notably, additional signals are observed near δ_C=145 ppm, which spectral analysis suggests may arise from heterocyclic compounds formed during the reaction, such as nitrogen-containing heterocycles including pyridine and quinoline derivatives. This interpretation is consistent with the ^{1}H-^{15}N HMBC data. However, these signals exhibit relatively low intensity, likely due to substitution at the ortho-position relative to the heteroatom in these heterocyclic structures[29]. Such substitution would hinder the observation of heteronuclear coupling between the nitrogen-adjacent carbon and hydrogen atoms, as illustrated in Figure 5. In high-field spectra, the signal distribution is broader and more complex compared to that in low-field spectra. Empirical evidence indicates that these signals arise from alkyl groups, implying the presence of a significant number of alkyl substituents, including those attached to aromatic rings and various aliphatic chains. Furthermore, nitrogen-rich tar was subjected to ^{1}H-^{13}C HMBC analysis, as shown in Figure 6，which also revealed highly complex signal patterns. This complexity is not surprising, as nitrogen-rich tar constitutes a highly heterogeneous mixture with highly diverse hydrogen and carbon chemical environments. However, the coupling signals of pyridine and quinoline classes can still be found in the figure. As can be seen from Figure 6, there are more coupling signals of H atoms in the high field and C atoms in the low field. This also indicates that the ortho-position of N atoms is mainly replaced by alkyl groups, which is consistent with the analysis results of ^{1}H-^{15}N HMBC, thereby further demonstrating the accuracy of the experiment.

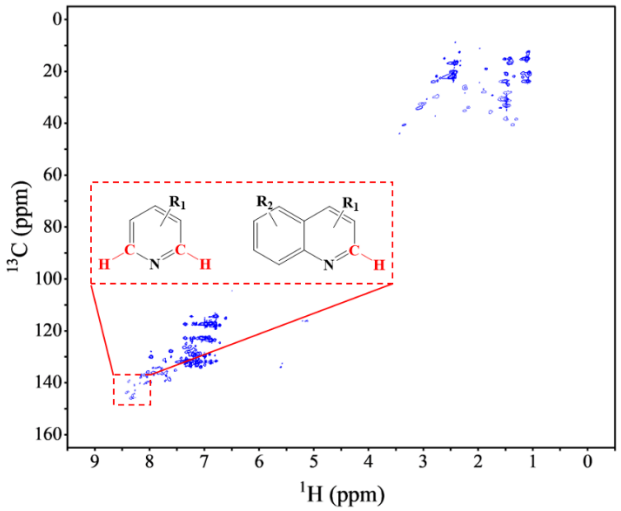

Figure 5. ^{1}H-^{13}C HSQC spectrum of nitrogen-rich tar (The compound structure shown here is the coupling signals of H and N in pyridine and quinoline types.)

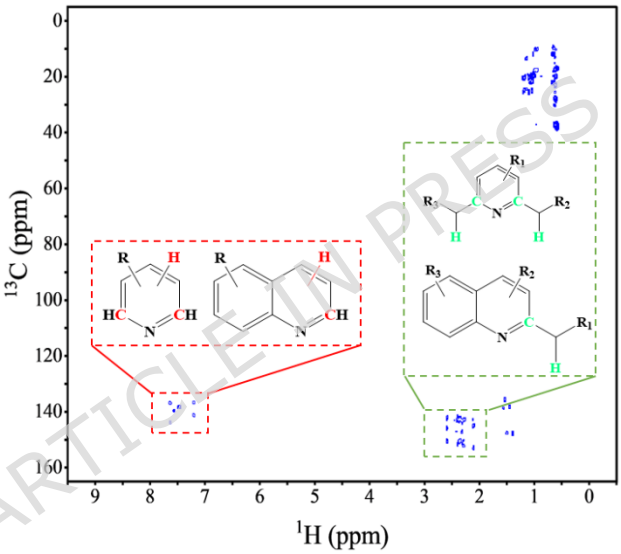

Figure 6. ^{1}H-^{13}C HMBC spectrum of nitrogen-rich tar (The compound structure shown here is the coupling signals of H and N in pyridine and quinoline types.)

GC/MS Analysis

Gas chromatography–mass spectrometry (GC/MS) is one of the most sensitive analytical techniques for the detection of nitrogen-containing compounds in tar[30]. It enables the determination of whether ^{15}N labeling occurs in tar during the co-pyrolysis of oil-rich coal and $^{15}NH_4Cl$ by monitoring m/z shifts. In nitrogen-containing compounds, the presence of a single ^{15}N atom leads to an m/z increase of 1 compared to ^{14}N, while the presence of two ^{15}N atoms results in a 2-unit increment, with this pattern scaling proportionally. However, compared with NMR, GC/MS poses significant challenges in analyzing isomers. Nevertheless, GC/MS analysis can still be adopted to further verify the accuracy of the experiment. Previous studies by our research group have shown that, under the operating conditions of this pyrolysis apparatus, the reactant ratio and reaction duration only affect the concentration of nitrogen-containing compounds in the tar, without altering their chemical species. In contrast, temperature variations significantly influence the diversity of nitrogen-containing compounds. Experimental results indicate that the optimal conditions for maximizing both coal tar yield and the diversity of nitrogen compounds are achieved at a pyrolysis temperature of 600 °C, with a reactant ratio of oil-rich coal to NH_4Cl of 1:3, and a reaction time of 3-4 minutes. As shown in Figure 7, the total ion chromatogram (TIC) displays the co-pyrolysis results of oil-rich coal with NH_4Cl and $^{15}NH_4Cl$. The two chromatograms exhibit identical profiles. Further

analysis of all detected peaks revealed corresponding m/z shifts at 27 distinct positions, indicating the presence of 27 nitrogen-containing compounds. Table 2 lists 27 nitrogenous compounds identified through the NIST database, including their respective retention times, relative abundances and based on the nuclear magnetic resonance signals of the standard nitrogen-containing compounds in Table 1, it can be inferred which quadrant the signal of this compound falls into. The experimental results initially confirm the complete feasibility of utilizing ^{15}N labeling during the co-pyrolysis process[31]. Moreover, the full substitution of ^{14}N by ^{15}N during the labeling process indicates complete isotopic incorporation. This method provides assistance for the subsequent verification of the reaction mechanism. As shown in Table 2, the ^{1}H-^{15}N HMBC signals of the 27 compounds predicted mostly lie in the first and fourth quadrants, which is basically consistent with the ^{1}H-^{15}N HMBC signals of the actual nitrogen-rich tar. The 27 nitrogen-containing compounds were classified into four categories: aromatic amines, aliphatic amines, five-membered nitrogen heterocycles (N-5), and six-membered nitrogen heterocycles (N-6). Their relative proportions were determined using the area normalization method, and the distribution is presented in Figure 8. Analytical data show that nitrogen heterocycles represent the dominant form of nitrogenous compounds (88.3%), whereas amines account for only 11.7%. Among all compound classes, five-membered nitrogen heterocycles exhibit the highest relative abundance. Comparative analysis against the NIST 14 database revealed that the five-membered heterocyclic compounds are mainly composed of pyrroles, imidazoles and other derivatives, such as No. 1, 3, 16, 26, and 27 in Table 2. Their common feature is that they are not composed of a single nitrogen heterocyclic ring, but are connected with many other groups. The most crucial point is that alkyl groups are attached to the α and β positions of the N atom, causing the originally low-field signal to shift to a high-field position. For example, the 2,2,5,5-tetramethyl-4-ethyl-3-imidazoline-1-oxyl of No.3. However, for the six-membered nitrogen heterocycles, the situation becomes more complicated. For the piperidine ring, the signals are mainly concentrated in the first quadrant, such as No. 7, 14, and 25 in Table 2. For the nitrogen heterocycles in the aromatic system, the signals are mostly located in the fourth quadrant, which is consistent with the above reasons. There are many alkyl groups attached to the aromatic ring, such as No. 8, 18, 21, and 27 in Table 2, etc. Among them, the most notable is that the peak of compound 6-methylquinoline 6 was accurately found. Since the mass spectra of methylquinoline are almost the same, by comparing the retention time of the standard sample of 6-methylquinoline, both show signals at 10.747 min[16], and this is highly consistent with the results of ^{1}H-^{13}C HSQC, ^{1}H-^{13}C HMBC, and ^{1}H-^{15}N HMBC, thereby further proving the accuracy of the experiment.

Table 2. Names, retention times, and relative abundances of 27 nitrogen-containing compounds.

No.	Most likely nitrogenous compounds	Retention time	Relative content [a]	Signal quadrant [b]
1	2-(tert-butyl)-1-methyl-1H-pyrrole	4.901	2.57	1,2
2	2,4,6-trimethylpyridine	5.343	0.59	3,4
3	2,2,5,5-tetramethyl-4-ethyl-3-imidazoline-1-oxyl	5.564	11.70	1
4	3-methyl-1,4,6,7-tetrahydro-pyrazolo[3,4-c]pyridin-5-one	6.810	0.97	4
5	4-methylbenzonitrile	6.870	0.81	No
6	2-Methylindoline	7.091	0.33	1
7	2,2,6,6-tetramethylpiperidin-4-one	7.211	10.97	1
8	4-hydroxy-1,6-dimethylpyridin-2(1H)-one	7.563	3.00	4
9	5-β,8-β-epoxy-3,5,8,8a-tetrahydro-1H-2-benzopyrrole	7.964	0.13	3
10	3,5-dimethylbenzaldehyde thiocarbamoylhydrazone	8.497	0.19	1
11	3-methylcyclohex-2-en-1-one O-methyl oxime	8.738	0.42	1
12	4-((isopropylimino)methyl)-N,N-dimethylaniline	9.180	0.20	1,2

13	2,2,6,6-tetramethylpiperidin-4-one O-acetyl oxime	9.451	1.24	1
14	5-(piperidin-1-yl)furan-2-carbaldehyde	9.692	1.26	1
15	3-ethyl-5,6,7,8-tetrahydroquinoline	9.973	0.24	4
16	7-[2,2-dimethoxy-1-propyl]- pyrrolizin-1-one	10.074	0.38	1
17	6-methylquinoline	10.747	2.10	3
18	4-(2,6,6-Trimethyl-cyclohex-1-enyl)-but-3-en-2-one oxime	11.098	1.04	4
19	2-acetyldecahydroisoquinoline-3-carbonitril	11.972	0.10	4
20	8-ethyl-2-methyl-4-quinolinol	12.534	0.14	4
21	12-azabicyclo[9.2.2]pentadeca-1(14),11(15)-dien-13-one	12.936	2.47	4
22	6,7,8,9-tetrahydro-5-methylisothiazolo[5,4-c]isoquinolin-1(2H)-one	13.066	1.14	4
23	1-[3-(3,3-Dimethyl-but-1-ynyl)-2,2-dimethyl-cyclopropyl]-piperazine	13.187	1.66	4
24	9-amino-1,8-dimethyl-3,6-diazahomoadamantane	13.639	1.12	1
25	2-[2-(1-piperidyl)ethyl]- 2,4-benzoxazin-1-one	16.672	2.74	1
26	2-methyl-a-pyrrolidinopropiophenone	18.459	1.38	1
27	6,7-dichloro-5-[(1-ethylpyrrolidin-2-yl)methylamino]-1,3-dimethyl- pyrido[2,3-d]pyrimidine-2,4(1H,3H)-dione	19.645	16.20	1,3,4

[a] The result was obtained by calculating the ratio of the peak area of each component to the total peak area in the TIC graph of GC/MS.

[b] Based on the nuclear magnetic resonance signals of the standard nitrogen-containing compounds in Table 1, it can be roughly inferred that the signal of this compound falls in which quadrant.

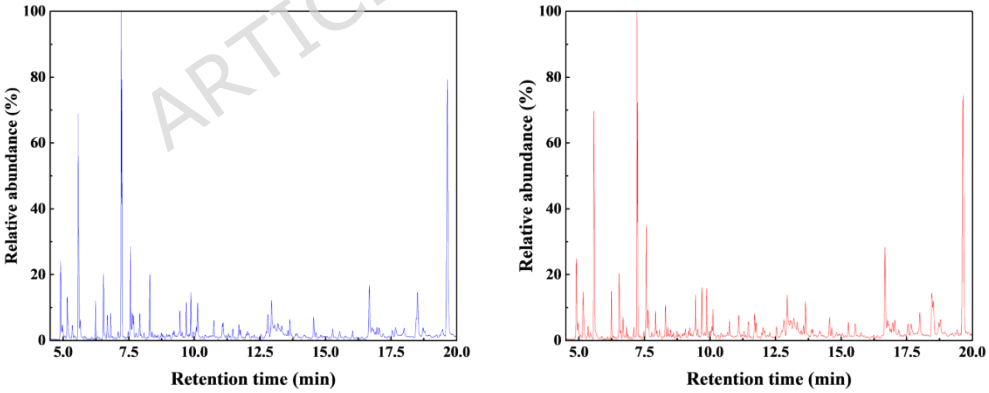

Figure 7. GC/MS chromatograms of tar obtained from the co-pyrolysis of Hongliulin oil-rich coal with NH_4Cl and $^{15}NH_4Cl$ (blue: NH_4Cl; red: $^{15}NH_4Cl$).

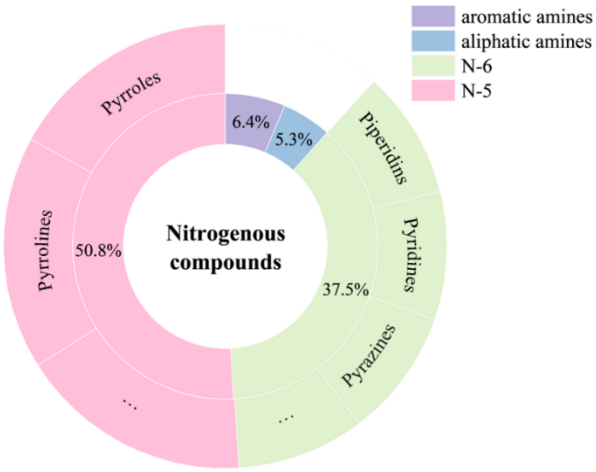

Figure 8. Classification and Content Analysis of Nitrogen-Containing Compounds in Tar Derived from the Co-Pyrolysis of Hongliulin Oil-Rich Coal with NH_4Cl.

Conclusion

This study established a method for rapidly screening the structures of nitrogen-containing compounds in complex products using ^{1}H-^{15}N HMBC NMR. The entire signal region was divided into four quadrants, and the types of nitrogen-containing compounds in each quadrant were analyzed and classified. This method was applied to the analysis of nitrogen-rich tar produced by the co-pyrolysis of Hongliulin oil-rich coal and ammonium chloride. Isotopic labeling with ^{15}N was employed to enhance NMR signal detection of nitrogenous compounds. The experimental results demonstrate that under optimized conditions (600 °C, a 1:1 mass ratio of Hongliulin oil-rich coal to ammonium chloride, and a pyrolysis duration of 3–4 minutes), the nitrogen-rich tar predominantly contains aliphatic amines, aromatic amines, five-membered nitrogen heterocycles, and six-membered nitrogen heterocycles. The five-membered nitrogen heterocycles predominantly consist of pyrrole and pyrroline derivatives, while the six-membered nitrogen heterocycles include piperidine, pyridine, and pyrazine compounds, among others. Furthermore, through the combined application of isotope labeling and GC/MS analysis, the identified nitrogen-containing compound types were found to be consistent with the results obtained from ^{1}H-^{15}N HMBC NMR. Quantitative assessment revealed that nitrogen heterocycles account for up to 88.3% of the four analyzed nitrogenous compound categories, all of which are thermally derived from biomass components present in coal. Finally, all data remain highly consistent, demonstrating the feasibility of employing ^{1}H-^{15}N HMBC NMR for the rapid screening of nitrogen-containing species in complex mixtures. This methodology provides valuable insights for the refined and high-value utilization of coal tar.

Methods

Experimental Materials: The oil-rich coal used in this study was obtained from the Hongliulin mining area. The coal samples were ground into fine powder and sieved to achieve a particle size of less than 200 mesh. All chemical reagents, including NH_4Cl, $^{15}NH_4Cl$, and standard samples of nitrogen-containing compounds, were purchased from Shanghai Macklin Biochemical Technology Co., Ltd. and used as received without further purification.

Co-pyrolysis Experiment: Co-pyrolysis experiments involving coal and nitrogen-containing compounds were conducted in a small-scale pyrolysis reactor[17]. A schematic diagram of the pyrolysis apparatus is presented in Figure 9. The quartz tube reactor used in the experiment had an outer diameter of 10 mm and an effective height of 400 mm. Prior to the experiment, 0.2 g of coal was accurately weighed and placed into a sealed stainless steel tube along with either 0.2 g of NH_4Cl or $^{15}NH_4Cl$. Quartz wool was then inserted at both ends of the stainless steel tube, which was subsequently mounted inside a quartz tube and secured[32]. The heating program was then initiated. The pyrolysis system was equipped with a thermocouple embedded within the electric heating furnace, and the reaction temperature was monitored and precisely controlled in real time using the temperature control system (TCS). Concurrently, a carrier gas (N_2) was introduced into

the reactor at an ultra-low flow rate, which was accurately regulated by a flowmeter to ensure maintenance of an inert atmosphere and continuous gas flow throughout the reactor. Based on previous research conducted by the research group, a pyrolysis temperature of 600 ℃ yielded relatively high product outputs. Therefore, all experiments were carried out at 600℃. As the pyrolysis products gradually flowed to the lower section of the quartz tube, the nitrogen-rich tar began to condense due to the lower temperature in that region. The uncondensed nitrogen-rich tar was collected in cooled tetrahydrofuran at the bottom. After the solvent was removed through drying, the residual products were analyzed and characterized.

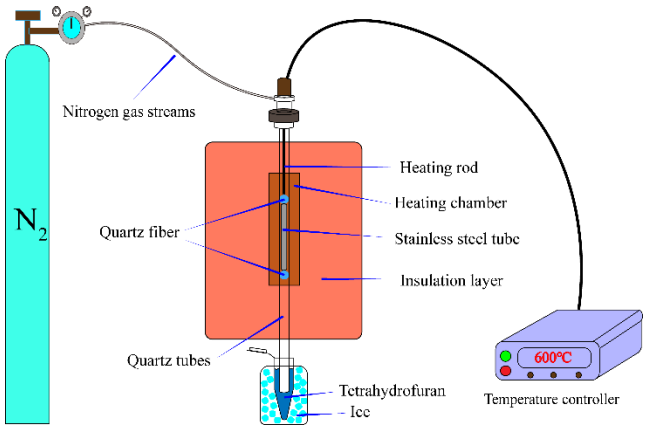

Figure 9. Schematic Diagram of the Pyrolysis Apparatus.

NMR Experiment: The NMR data were acquired using a Bruker Avance III HD spectrometer operating at 400 MHz, equipped with a PA BBO 400S1 BBF-H-D-05 Z SP probe, with the experimental temperature maintained at 298 K. A 50 mg sample of nitrogen-rich tar obtained after co-pyrolysis was dissolved in 500 μL of $CDCl_3$, thoroughly mixed, and then transferred into a 5 mm NMR tube. ^{1}H-^{13}C HSQC employs the HSQCEDETGPSISP pulse sequence, with NS=4, DS=32, and DR=22s; ^{1}H-^{13}C HMBC uses the HMBCETGPL3ND pulse sequence, with NS=4, DS=16, and DR =23s; ^{1}H-^{15}N HMBC employs the HMBCGP_15N pulse sequence, with NS=8, DS=16, and DR=23s.. All spectral data were processed using Bruker Topspin 4.1.1 software. Figure 9 presents a schematic diagram of the sample preparation and experimental procedure[33].

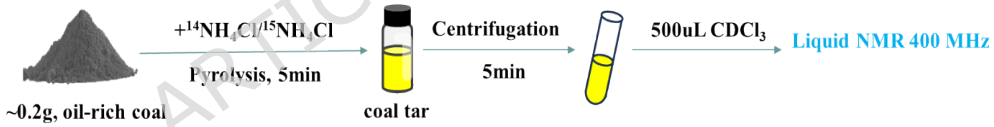

Figure 10. The sketchy diagram of sample preparation and experimental of NMR procedure.

GC/MS Experiment: The pyrolyzed products were introduced into the GC/MS system for analysis, with high-purity helium used as the carrier gas through an HP-5MS capillary column (30 m × 0.25 mm × 0.25 μm). The GC/MS split ratio was set at 50:1. The oven temperature program began at 80 ℃ with a 1-minute hold, followed by a heating rate of 20 ℃/min to 310 ℃, with a final hold of 4 minutes. Compound identification was carried out using gas chromatography–mass spectrometry by comparing the obtained spectra with the NIST 14 library. All experiments were conducted in triplicate, with reproducibility confirmed within the 95% confidence interval[34]. The schematic diagram of the GC/MS is presented in Figure 11.

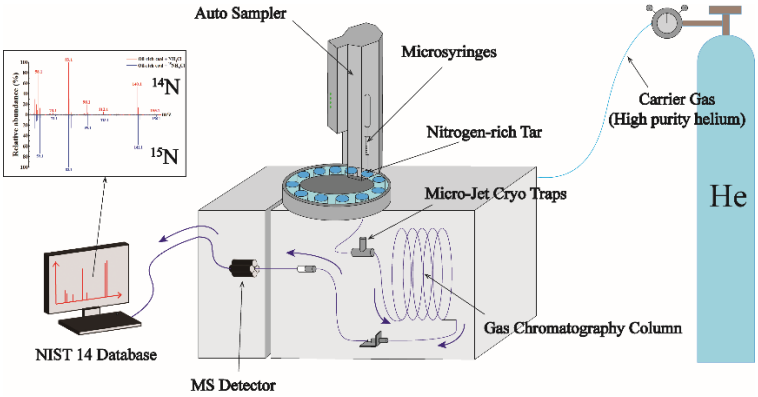

Figure 11. Schematic Diagram of the GC/MS.

References

1. Lam, S., Liew, R., Wong, Y., Yek, P., Ma, N., Lee, C. & Chase, H. Microwave-assisted pyrolysis with chemical activation, an innovative method to convert orange peel into activated carbon wit h improved properties as dye adsorbent. *Journal of Cleaner Production*. **162**, 1376-1387, DOI: https://doi.org/10.1016/j.jclepro.2017.06.131 (2017).

2. Wan, M., Chong, C., Lam, W., Anuar, T., Ma, N., Ibrahim, M. & Lam, S. Microwave co-pyrolysis of waste polyolefins and waste cooking oil: influence of N_2 atmosphere versus vacuum environ ment. *Energy Conversion and Management*. **171**, 1292-1301, DOI: https://doi.org/10.1016/j.enc onman.2018.06.073 (2018).

3. Bakker, A.T., Kotsogianni, I., Avalos, M. et al. Discovery of isoquinoline sulfonamides as alloster ic gyrase inhibitors with activity against fluoroquinolone-resistant bacteria. *Nature Chemistry.* **1 6**, 1462–1472. DOI: https://doi.org/10.1038/s41557-024-01516-x (2024).

4. Khaleel, C., Tabanca, N. & Buchbauer, G. α-Terpineol, a natural monoterpene: a review of its bi ological properties. *Open Chemistry*. **16**, 349–361. DOI: https://doi.org/10.1515/chem-2018-0040 (2018).

5. Roshan, M., Mirzazadeh, R., Tajmir-Riahi, A. et al. Rational design, synthesis, in vitro, and in-sil ico studies of pyrazole-phthalazine hybrids as new α-glucosidase inhibitors. *Scientific Reports*. **1 5**, 3744. DOI: https://doi.org/10.1038/s41598-025-87258-3 (2025).

6. Chen, P., Fang, Y., Wang, P., Gu, M., Luo, K. & Fan, J. The effect of ammonia co-firing on NO h eterogeneous reduction in the high-temperature reduction zone of coal air-staging combustion: Experimental and quantum chemistry study. *Combustion and Flame*. **237**, DOI: https://doi.org/1 0.1016/j.combustflame.2021.111857 (2022).

7. Jiao, A., Xu, H., Liu, F., Liao, X., Liu, J. & Jiang, X. Mechanistic study on the effect of ammonia c o-firing with pulverized coal on NO formation and reduction. *Chemical Engineering Science*. **28 2**, DOI: https://doi.org/10.1016/j.ces.2023.119306 (2023).

8. Jiang, K., Cao, L., Hao, Z., Chen, M., Cheng, J., Li, X., Xiao, P., Chen, L. & Wang, Z. Research pr ogress in design, synthesis and application of benzothiazole-based fluorescent probes. *Chinese Journal of Organic Chemistry*. **37(9)**, 2221-2236, DOI: https://doi.org/10.6023/cjoc201703041 (2 017).

9. Zhang, X., Song, Q., Liu, S., Sivaguru, P., Liu, Z., Yang, Y., Ning, Y., Anderson, E., de Ruiter, G. & Bi, X. Asymmetric dearomative single-atom skeletal editing of indoles and pyrroles. *Nature C hemistry*. **17(2)**, DOI: https://doi.org/10.1038/s41557-024-01680-0 (2024).

10. Liu, S., Yang, Y., Song, Q., Liu, Z., Lu, Y., Wang, Z., Sivaguru, P. & Bi, X. Tunable molecular editing of indoles with fluoroalkyl carbenes. *Nature Chemistry*. **16(6)**, DOI: https://doi.org/10.1 038/s41557-024-01468-2 (2024).

11. Ma. Q., Zuo, Y., Liang, Z. & Li, P. Separation and enrichment of polycyclic aromatic hydroc arbons and nitrogen heterocyclic aromatic compounds in high-temperature coal tar. *Modern Ch emical Research*. **3**, 51-53, DOI: https://doi.org/10.20087/j.cnki.1672-8114.2024.03.017 (2024).

12. Ding, X., Ren, X., Liu, W., Guo, L., Wang, S., Zhao, X. & Wang, Y. Research Progress on Intr insically Safe Synthesis Technology of Aniline and toluenediamine. *Chemical Industry and Engi neering*. **2**, 41, DOI: https://doi.org/10.13353/j.issn.1004.9533.20230807 (2024).

13. Ma, Z., Dong, X., Li, S., Liu, G., Xiao, R., Ju, C., Li, L., Guo, X., Zong, Z., Cong, X. & Wei, X. Molecular identification of nitrogen-containing aromatics for chemical separation from five frac tions distilled from a high temperature coal tar. *Journal of the Energy Institute*. **113**, DOI: https: //doi.org/10.1016/j.joei.2024.101534 (2024).

14. Ren, X., Yang, J., Duan, J., Feng, X., Zhang, Y., Liu, L., Tang, Y. & Zhou, X. Identification of organic components in coal tar by pressurized fluid extraction in conjunction with comprehensi ve two-dimensional gas chromatography/time-of-flight mass spectrometry. *Journal of the Energy Institute*. **120**, DOI: https://doi.org/10.1016/j.joei.2025.102073 (2025).

15. Wang, X., He, X., Wang, X. FTIR Analysis of the Functional Group Composition of Coal Tar Residue Extracts and Extractive Residues. *Applied Sciences-Basel*. **13(8)**, DOI: https://doi.org/1 0.3390/app13085162 (2023).

16. He, Y., Chen, F., Han, X. & Zhang, N. Conversion of methyl cinnamic acid into nitrogenous compounds during pyrolysis revealed using 15N isotopic labeling. *Journal of Analytical and App lied Pyrolysis*. **178**, DOI: https://doi.org/10.1016/j.jaap.2024.106408 (2024).

17. Krivdin, L. Recent advances in liquid-phase NMR of the coal-derived products. *Magnetic Re sonance in Chemistry*. **62(11)**, 775-802, DOI: https://doi.org/10.1002/mrc.5476 (2024).

18. Gao, X., Ma, M., Pedersen, C., Liu, R., Zhang, Z., Chang, H., Qiao, Y. & Wang, Y. Interaction s between PAMAM-NH_2 and 6-Mercaptopurine: Qualitative and Quantitative NMR studies. *Che mistry-An Asian Journal*. **16(22)**, 3658-3663, DOI: https://doi.org/10.1002/asia.202100771 (202 1).

19. Ma, J., Ye, Q., Green, R., Gurak, J., Ayers, S., Huang, Y. & Miller, S. Overcoming NMR line broadening of nitrogen containing compounds: A simple solution. *Magnetic Resonance in Chem istry*. **62(3)**, 198-207, DOI: https://doi.org/10.1002/mrc.5432 (2024).

20. Ramirez, B., Durst, M., Lavie, A., Caffrey, M. NMR-based metabolite studies with ^{15}N amino acids. *Scientific Reports*. **9**, DOI: https://doi.org/10.1038/s41598-019-49208-8 (2019).

21. Kiraly, P., Kern, N., Plesniak, M., Nilsson, M., Procter, D., Morris, G. & Adams, R. Single-Sc an Selective Excitation of Individual NMR Signals in Overlapping Multiplets. *Angewandte Chemi e - International Edition*. **60(2)**, 666-669, DOI: https://doi.org/10.1002/anie.202011642 (2020).

22. Deng, J., Lang, W., Zhu, Z., Huang, Y., Liu, H., Liu, J. & Yuan, S. Porous Nitrogen-Doped Ca rbon Ni Nanocatalysts for H_2-Free and Solvent-Free Pyrolysis of Real Coal Tar to Light Aromati cs (C_6-C_{10}). *ACS Catalysis Journal*. **15(15)**, 12800-12815, DOI: https://doi.org/10.1021/acscatal. 5c03607 (2025).

23. Zhang, L., Wen, X., Kong, T., Zhang, L., Gao, L., Miao, L. & Li, Y. Preparation and mechanis m research of Ni-Co supported catalyst on hydrogen production from coal pyrolysis. *Scientific Reports*. **9**, DOI: https://doi.org/10.1038/s41598-019-44271-7 (2019).

24. Cao, M., E, R., Yuan, C., Rosendahl, L., Zhang, Y., Xu, C., Wu, Y., Kong, D., Wang, Y., Li, J. & Liu, Z. Green coal and lubricant via hydrogen-free hydrothermal liquefaction of biomass. *Nat ure Communications*. **16(1)**, DOI: https://doi.org/10.1038/s41467-025-56037-z (2025).

25. Huang, J., Qiao, Y., Liu, H., Wang, B., Wang, Z., Yu, Y. & Xu, M. Effect of Torrefaction on Ph ysicochemical Properties and Steam Gasification Reactivity of Chars Produced from the Pyrolys is of Typical Food Wastes. *Energy & Fuels*. **34(12)**, 15332-15342, DOI: https://doi.org/10.1021/ acs.energyfuels.0c03217 (2020).

26. Ghani, R., Boostani, F. & Iranshahi, D. Analysis of the Combined Ammonia Production and Cyclohexane Dehydrogenation by a Novel Bifunctional Reactor. *Energy & Fuels*. **33(7)**, 6717-6 726, DOI: https://doi.org/10.1021/acs.energyfuels.9b01088 (2019).

27. Zhou, Y., Li, L., Jin, L., Zhu, J., Li, J., Li, Y., Fan, H. & Hu, H. Effect of functional groups on volatile evolution in coal pyrolysis process with in-situ pyrolysis photoionization time-of-flight m ass spectrometry. *Fuel.* **260**, DOI: https://doi.org/10.1016/j.fuel.2019.116322 (2020).

28. Ghysels, S., Verwaeren, J., Heeres, H., Rohrbach, L., Backx, S., Mangelinckx, S. & Ronsse,

F. Exploring Image Processing Tools To Unravel Complex ^{1}H-^{13}C Heteronuclear Single-Quantum Correlation Nuclear Magnetic Resonance Spectra: A Demonstration for Pyrolysis Liquids. *Energy & Fuels*. **37(6)**, 4446-4459, DOI: https://doi.org/10.1021/acs.energyfuels.2c04100. (2023)

29. Wang, Y., Fan, A., Cohen, R., Dal Poggetto, G., Huang, Z., Yang, H., Martin, G., Sherer, E., Reibarkh, M. & Wang, X. Unequivocal identification of two-bond heteronuclear correlations in natural products at nanomole scale by i-HMBC. *Nature Communications*. **14(1)**, DOI: https://doi.org/10.1038/s41467-023-37289-z (2023).

30. Liu, H., He, L., Wang, W., Wang, L., Ma, D., Wang, J., Yao, Q. & Sun, M. Determination of boiling point distribution by TG using a novel crucible and comparison with true boiling point distillation and simulated distillation by GC-MS and Py-GC/MS. *Chemical Engineering Journal*. **484**, DOI: https://doi.org/10.1016/j.cej.2024.149481 (2024).

31. Hiroaki S., Hajime O., Ryo H., Shin T., Makoto K. & Arimitsu U. Polymer/silicate Interaction in Nylon 6-Clay Hybrid Studied by Temperature Programmed Pyrolysis Techniques. *Polymer Journal*. **38**, 171–177, DOI: https://doi.org10.1295/polymj.38.171 (2006).

32. Bisen, D., Chouhan, A., Sarma, A., Rajamohan, S., Elumalai, P., Balasubramanian, D. & Cherie, A. Thermogravimetric analysis of rice husk and low-density polyethylene co-pyrolysis: kinetic and thermodynamic parameters. *Scientific Reports*. **14(1)**, DOI: https://doi.org10.1038/s41598-024-82830-9 (2025).

33. Korb, J. Multiscale nuclear magnetic relaxation dispersion of complex liquids in bulk and confinement. *Progress in Nuclear Magnetic Resonance Spectroscopy*. **104**, 12-55, DOI: https://doi.org10.1016/j.pnmrs.2017.11.001 (2018).

34. Hossain, M., Khalekuzzaman, M., Kabir, S., Islam, M. & Bari, Q. Production of light oil-prone biocrude through co-hydrothermal liquefaction of wastewater-grown microalgae and peat. *Journal of Analytical and Applied Pyrolysis*. **161**, DOI: https://doi.org/10.1016/j.jaap.2021.105423 (2022)

Funding

This research was funded by the National Natural Science Fundamental Project (No. U24A20552, 32202164), Scientific Research Program Funded by Shaanxi Provincial Education Department (No.21JK0772), Xi'an Science and Technology Plan Project (No. 23NYGG-0068) for the financial support.

Author contributions statement

Y.Z., F.C. and Z.L. conceived the project and designed the research. P.C., B.S. and G.L. performed NMR experiment. N.W., H.T. and A.Z. provided co-pyrolysis of rich oil coal. G.S. and A.Z. provided GC-MS analysis. X.H. and B.S carried out statistical analyses and structural analysis. P.C., Q.W. wrote and revised the manuscript.